通过循环深冷处理策略实现 AlCoCrFeNi2.1 共晶高熵合金的位错-析出相协同强化

柳成昊 ^{1,2},张斯若 ^{1,2},齐浩 ^{1,2},武皓恺 ^{1,2},刘子墨 ^{1,2},**曲迎东 ^{2,3},*李广龙 ^{1,2}

- (1. 辽宁省高校轻金属材料与工程重点实验室,辽宁省沈阳市,110870;
- 2. 辽宁省高校轻金属材料与工程重点实验室,辽宁省沈阳市,110870;
 - 3. 沈阳航空航天大学,辽宁省沈阳市,110136)

**通讯作者: 曲迎东, 男, 教授, 博士。E-mail: quyingdong@163.com

*通讯作者: 李广龙, 男, 副教授, 博士。E-mail: liguanglong1990@163.com

摘 要:本文提出了循环深冷处理(CDCT)AlCoCrFeNi_{2.1}共晶高熵合金的优化策略。利用 SEM 、TEM 、EBSD 对不同循环深冷处理时间的 AlCoCrFeNi_{2.1}共晶高熵合金的微观结构进行观察与分析。使用万能试验 机进行拉伸试验,研究了不同 CDCT 对试样力学性能的影响。经分析发现,随着 CDCT 次数增加,试样中的位错密度存在增加的趋势。同时在 B2 相中产生 BCC 析出相,在 FCC 中析出 L1₂ 析出相。两种析出相共同作用作为位错开动的源头提升试样塑性。高密度位错与析出相共同作用,实现 CDCT 同时提升 AlCoCrFeNi_{2.1} 共晶高熵合金极限抗拉强度和延伸率。结果表明,经 CDCT-4 后,合金内部位错密度增加,同时产生高密度 BCC 与 L1₂ 双析出相,作为位错开动源。室温下合金强塑性同时增强。抗拉强度达到 1107.18 MPa ,相比铸态提高 13.64%。塑性达到 24.21%,相比铸态提高 23.33%。

关键词:循环深冷处理;高熵合金;位错;析出相

Realizing The Dislocation-precipitate Synergy Strengthening Of AlCoCrFeNi2.1 Eutectic High-entropy Alloy Through Cyclic Deep Cryogenic Treatment Strategy

Liu Cheng-hao ^{1,2}, Zhang Si-ruo ^{1,2}, Qi Hao ^{1,2}, Wu Hao-kai ^{1,2}, Liu Zi-mo^{1,2}, **Qu Ying-dong ^{2,3}, *Li Guang-long ^{1,2}

- (1. School of Materials Science and Engineering, Shenyang University of Technology, Liaoning Shenyang, 110870, China;
- 2.Technical Innovation Center for Lightweight and High-Performance Metal Materials of Liaoning Province, Liaoning Shenyang, 110870, China; 3.Shenyang Aerospace University, Liaoning Shenyang, 110136, China)

Abstract: This article presents an optimization strategy for the cyclic deep cryogenic treatment (CDCT) of the AlCoCrFeNi2.1 eutectic high-entropy alloy. The microstructure of the AlCoCrFeNi2.1 eutectic high-entropy alloy subjected to different CDCT durations was observed and analyzed using SEM, TEM, and EBSD. Tensile tests were conducted using a universal testing machine to study the effects of different CDCTs on the mechanical properties of the samples. Analysis revealed that with an increase in the number of CDCT cycles, there is a tendency for the dislocation density within the samples to increase. Concurrently, BCC precipitate phases are formed in the B2 phase, and L12 precipitate phases are formed in the FCC structure. The combined action of both precipitate phases serves as the dislocation activation source, enhancing the plasticity of the samples. The collaboration of high dislocation density and precipitate phases results in a simultaneous increase in the ultimate tensile strength and elongation of the AlCoCrFeNi2.1 eutectic high-entropy alloy through CDCT. The results show that after CDCT-4, the dislocation density inside the alloy increases, while high-density BCC and L12 co-precipitate phases are formed, serving as dislocation activation sources. The alloy demonstrates significantly enhanced strength and plasticity at room temperature, with tensile strength reaching 1107.18 MPa, which is an increase of 13.64% compared to the cast state. The plasticity reaches 24.21%, which is an improvement of 23.33% compared to the cast state.

Keywords: cyclic deep cryogenic treatment (CDCT); high-entropy alloy; dislocation; precipitate phases

1 Introduction

The development of high-entropy alloys has fundamentally broken the traditional concepts of alloy design^[1-2]. Their multiphase characteristics provide significant potential for regulating microstructures, deformation mechanisms, and mechanical properties. The design of materials with high strength and high ductility is the central focus of engineering materials and has attracted extensive scientific research. Some refractory high-entropy alloys exhibit high strength but low ductility and poor flowability, making them unsuitable for large-scale part fabrication. In 2014, Lu Yiping^[3] proposed the AlCoCrFeNi_{2.1} high-entropy alloy, a type that forms a regular eutectic structure during solidification, consisting alternating layers or fibrous structures of soft phase (FCC phase) and hard phase (such as BCC/B2 phase). Eutectic high-entropy alloys feature fewer casting defects (e.g., shrinkage pores, segregation) and can be directly cast into large components. However, their capacity for ductile deformation under high-stress service conditions is insufficient, leading to rapid initiation and propagation of cracks, thus limiting the widespread application of eutectic high-entropy alloys in specialized service environments. Dislocation strengthening can serve as an effective means to enhance the mechanical properties of high-entropy alloys; the movement of dislocations can be effectively hindered by precipitate phases, grain boundaries, and other lattice defects, resulting in higher stresses resisting deformation. Among these, L₁₂-type high-entropy alloys, by introducing high-density compact interfaces that impede dislocation slip, exhibit outstanding mechanical properties at both low and high temperatures, becoming one of the hot research topics in high-entropy alloys in recent years^[4-5]. Among the high-entropy alloys currently studied, the L12 reinforced HEAs with face-centered cubic structures show remarkable potential terms ofstrength-ductility synergy, making them favored in the field of additive manufacturing. However, due to the need to prevent excessive local stress that affects service life, high-entropy alloys produced by additive manufacturing often require prolonged aging heat treatment. This leads to a significant reduction in dislocation strengthening effects, with dislocation density notably decreasing above 350°C. Benefiting from recent research, deep cryogenic treatment is a non-destructive strengthening method. This process involves using liquid nitrogen as a cooling medium to

instantaneously cool the alloy to well below room temperature (-196 °C). Due to the accumulation of micro-stresses generated by alternating heating and cooling cycles, it has been proven to effectively promote the formation of stacking faults or deformation twins. This treatment can significantly improve the grain boundary distribution, dislocation density, and the number of precipitated phases in high-entropy alloys, thereby enhancing mechanical properties. In recent years, our research group has demonstrated that deep cryogenic treatment (DCT) is a simple and effective method to enhance the mechanical performance of Al_xCrFe₂Ni₂ series high-entropy alloys. Previous studies by our group indicated that after subjecting the Al_xCrFe₂Ni₂ series high-entropy alloys to DCT for varying durations, alloys exhibited different densities of dislocations and precipitated phases. Thanks to dislocation strengthening and precipitation strengthening, the compressive strength of Al_xCrFe₂Ni₂ high-entropy significantly increases following alloys cryogenic treatment. Furthermore, the deep cryogenic treatment process is simpler and more economical compared to traditional heat treatment processes^[6-8]. This study proposes a cyclic deep cryogenic heat treatment method, involving repeated low-temperature cooling and reheating, systematically investigating the microstructural effects of continuous deep cryogenic treatment (CDCT) on the AlCoCrFeNi_{2.1} high-entropy alloy prepared by vacuum arc melting, in comparison to a single DCT with the same duration at low temperature, as well as the enhancement in room temperature tensile strength and ductility. The findings from this experiment on the influence of CDCT on the mechanical properties of eutectic high-entropy alloys offers a new strategy for achieving cooperative dislocation-precipitation strengthening AlCoCrFeNi_{2.1} EHEAs. This research provides valuable reference for expanding effective non-destructive methods to strengthen the mechanical performance of high-entropy alloy castings.

2 Experimental

Under the protection of argon atmosphere, non-self-consumable vacuum arc melting (BTFJ21-03, BoTong LiHua) was used to prepare button-type ingots with the nominal composition of AlCoCrFeNi_{2.1} (at. %), and the Zr ingots were pre-melted to absorb trace amounts of oxygen. The metal raw material is Al, Co, Cr, Fe and Ni blocks with a purity of at least 99.9 wt.%. Each high-entropy alloy ingot is flipped and melted at least 4 times, and electromagnetic stirring is

turned on 30s before the end of each melting to ensure the uniformity of chemical composition. The Cyclic Cryogenic Treatment (CDCT) process uses a sealed liquid nitrogen tank and a vacuum tube furnace (KSL-1200X, KeJing) with an outer insulating layer that keeps the temperature constant at 77 K. Firstly, the samples melted by vacuum arc were cooled to room temperature under argon atmosphere, then the polished surface was taken out to be bright, placed in a liquid nitrogen tank and soaked for 12 h, immediately heated to room temperature in a water bath and kept

for 0.5 h, and then low-temperature heat treatment was carried out in a vacuum tube furnace, the temperature was set to 503 K, kept warm for 2 h, and the water bath was immediately taken out and heated to room temperature. The entire "cold-hot" process is recorded as a "single cycle", as shown in Figure 1(b). In this study, samples were designed in five states: 0-4 cycles of CDCT, corresponding to the total time of low temperature immersion at 0 h, 12 h, 24 h, 36 h and 48 h, respectively. Each group of samples was named as-cast, CDCT-1, CDCT-2, CDCT-3 and CDCT-4.

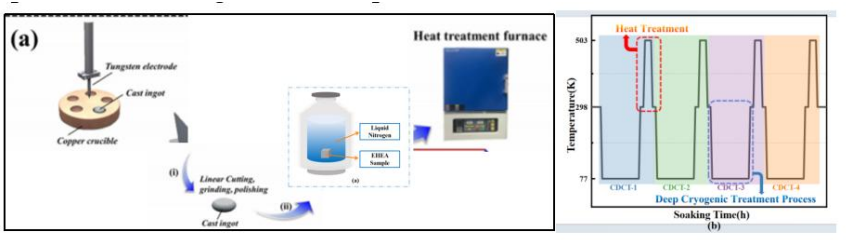


Fig. 1: Schematic diagram of a CDCT device (a) and flowchart of the CDCT process (b)

X-ray diffraction (XRD, Shimadzu 7000) equipped with a Cu-Ka target material was employed to characterize phase formation and crystal structure, with data collected in the 20°-100° range at a scanning rate of 2° min-1. The surface of the samples after CDCT was mechanically polished using SiC sandpaper. Subsequently, electro-polishing (Naibo EP-06) was performed to remove the scratch layer induced by previous mechanical grinding, using an etching solution composed of 10 vol% perchloric acid and 90 vol% ethanol. Scanning electron microscopy (SEM, ZEISS Gemini 300), energy-dispersive X-ray spectroscopy (EDS, Oxford Aztec), and electron backscatter diffraction (EBSD) detectors were utilized, with a scanning step of 0.7 µm and a collection speed of 40 Hz to obtain EBSD images in a 250 μm × 200 um area for characterization of grain size and orientation features. Transmission electron microscopy (TEM, JEM-2100) was used to investigate the microstructure of the cast state and CDCT-treated samples, further characterizing the morphology, grain, and structure. For the preparation of TEM samples, TEM foils were cut from the samples and mechanically polished to 45-50µm, followed by ion thinning (Gatan 691) to achieve electron transparency. A tensile test was conducted at room temperature using an electronic universal testing machine (MTS-E45) with an initial strain rate of 1×10^{-3} s⁻¹. Before the tensile test, the samples were mechanically polished and polished using diamond paste. The thickness, width, and gauge length of the tensile samples prepared by electrical discharge machining (EDM) were 2.0 mm, 4.0 mm, and 7.0 mm, respectively, as shown in Figure 1(c). Each sample was tested at least three times under each condition to ensure result consistency. During the tensile process, the real-time stress-strain distribution was recorded using a mechanical extensometer. The fracture morphology of each set of EHEA samples was examined after the tensile test using scanning electron microscopy (SEM, ZEISS Gemini 300).

Tab.1 Nominal composition of the as-cast AlCoCrFeNi2.1 high entropy alloy

Element	Al	Co	Cr	Fe	Ni
Atomic Weight	26.82	58.93	51.99	55.85	58.69
Atomic Percent (%)	16.40	16.40	16.40	16.40	34.40
Mass Percent (%)	8.52	18.60	16.41	17.62	38.85

3 Results and discussion

3.1 Microstructure characterization

Figure 2(a) shows the XRD spectra of the AlCoCrFeNi_{2.1} high-entropy alloy before and after CDCT. Clearly, all spectra only display the typical dual-phase FCC B2 structure. Due to the very close lattice constants, the XRD spectra demonstrate the coexistence of FCC and L1₂ phases, as well as the coexistence of B2 and BCC phases in the AlCoCrFeNi_{2.1} EHEA, which is consistent with the cast state, indicating that no new phase was formed during CDCT. Notably, as seen in Figure 2(b), the 20 value of the (111) peak increases, suggesting a slight decrease in interplanar spacing with increasing CDCT cycles. Other peaks such as (200), (220), and (311) exhibit the same trend. The decrease in interplanar spacing indicates that the CDCT results in an increase

of the internal compressive residual stress of samples prepared by vacuum arc melting, because CDCT induces stress rather than relieving it^[9]. Our previous research found that compared to simple DCT, the degree of peak shift is reduced, suggesting that the combination of CDCT with low-temperature heat treatment can mitigate residual stress, preventing excessive localized residual stress and avoiding it becoming a source of crack propagation during the tensile process. Furthermore, using equation (1) for peak fitting of the (220) peak, the lattice parameters of the FCC/L12 and B2/BCC phases were determined, as shown in Figure 2(c). It is evident that with the increase of deep cooling treatment time, the degree of mismatch between the FCC and L1₂ phases gradually decreases[10].

$$d = \frac{a}{\sqrt{h^2 + k^2 + l^2}}$$
 (1)

In the formula, 'a' represents the lattice constant (the edge length of the cubic crystal system). 'h', 'k',

and 'l' are Miller indices that indicate the direction of the crystal planes. Based on the XRD spectrum and the Williamson-Hall method, the dislocation density values of the four samples after CDCT were calculated. It can be observed that, compared to the cast state, the dislocation density of samples after CDCT is significantly higher, with CDCT-1 exhibiting a dislocation density of approximately 3.65 × 1014m-2, and CDCT-2 showing a dislocation density of about 5.71 × 1014m-2. Furthermore, after undergoing 3 to 4 rounds of CDCT, the dislocation density of the samples approaches saturation, reaching as high as approximately 8.23 × 1014 m-2.

The SEM image in Fig. 3 shows the microstructure of as-cast AlCoCrFeNi2.1 EHEA. The eutectic structure with lamellar structure in Fig. 3(a) is composed of FCC phase and B2 phase alternately. The non-eutectic structure of coarse dendrite structure contains short rod-like B2 phase. EDS analysis shows that the B2 phase is rich in Al and Ni, and the FCC phase is rich in Fe, Co and Cr.

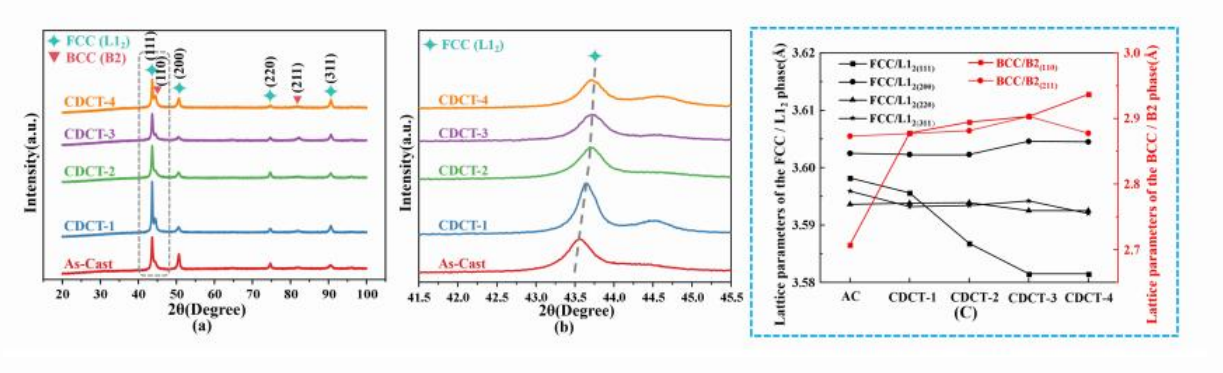


Fig. 2. XRD patterns and lattice parameter variation diagram: (a) XRD patterns of cast and different CDCT times for AICoCrFeNi2.1 EHEA; (b) local magnification of XRD pattern; (c) lattice parameters of various phases in EHEA under different CDCT time

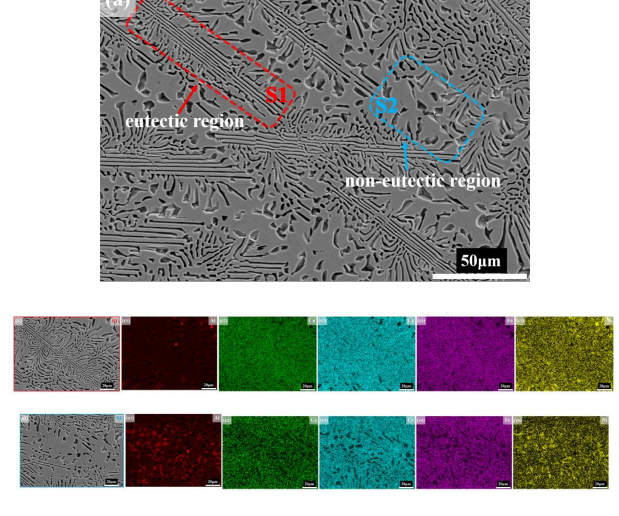


Fig. 3. Microstructure and element distribution in the as-cast AlCoCrFeNi2.1 EHEA: (a) SEM images of the as-cast AlCoCrFeNi2.1 EHEA; (b-c) element distribution of Al, Co, Cr, Fe and Ni in AlCoCrFeNi2.1 EHEA

In order to explore the effect of CDCT on the microstructure, the EBSD characterization of the study area before and after CDCT treatment was carried out, and the relevant results were given. By comparing Figure 4, the Kernel Average Misorientation (KAM) plot shows that for CDCT samples, the high KAM values are mainly concentrated near grain boundaries, indicating a significant residual strain between adjacent grains. Obviously, the KAM value within the crystal increases significantly after the number of CDCT cycles increases (green is the area with high KAM and blue is the area with low KAM). It can be observed that the increase in the number of CDCTs will significantly increase the density of crystal defects. The average KAM value can be used to evaluate the dislocation density, and the average KAM value of 0.08° for the as-cast sample is due to the rapid solidification of the vacuum arc melting under the action of copper pans and water cooling, resulting in a

small amount of dislocation. The average KAM values of CDCT-1~CDCT-4 samples were 0.17°, 0.23°, 0.36° and 0.37°, respectively. As shown in Figure 4 (b1-b2), the microstructure of the X-Y plane region in the as-cast sample and the sample after different cycles of CDCT consists of a mixture of columnar and near-equiaxed crystals, and no other subcrystalline

phases were detected. It can be found that although CDCT does not significantly change the morphology and size of the grains, it does lead to different degrees of changes in grain orientation, which indicates that CDCT introduces microstress and microstrain, and the microstress and microstrain also increase gradually with the increase of the number of cycles.

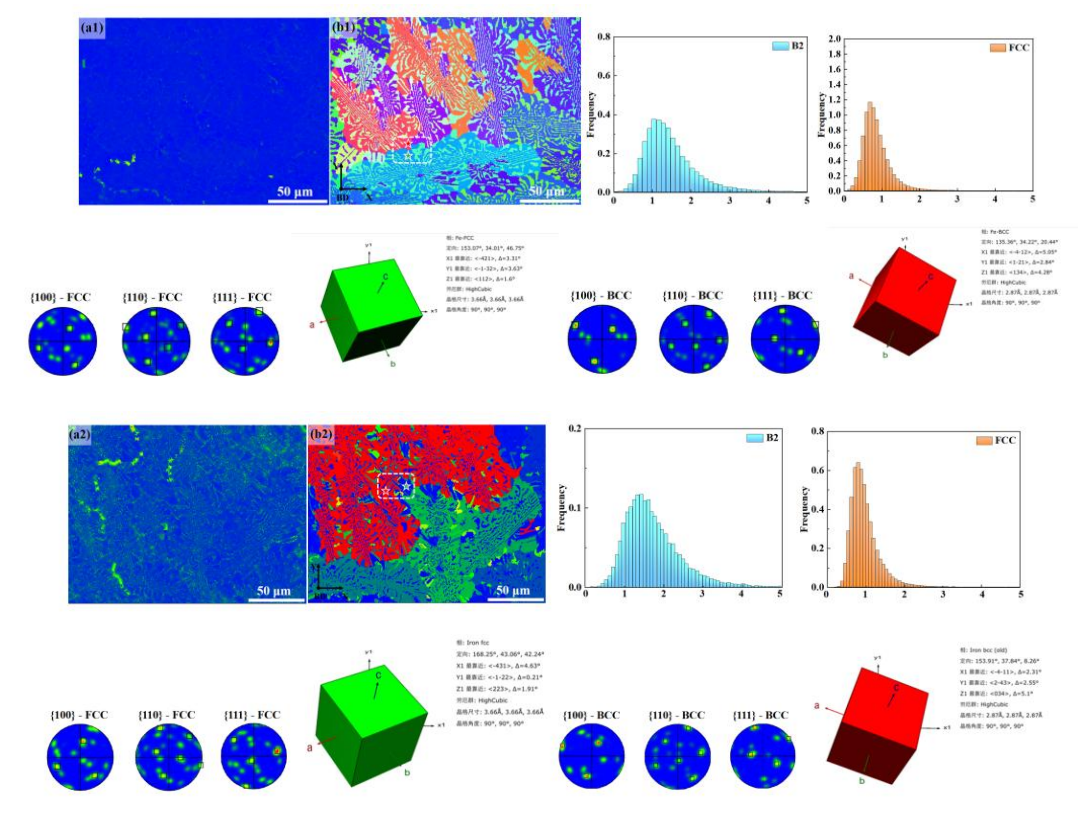


Fig. 4. EBSD images of the microstructure of AlCoCrFeNi2.1 EHEA as cast and CDCT: (a1-a2) KAM images; (b1-b2) IPF phase diagram of different alloys; (c1-c2) KAM data histogram and average KAM value

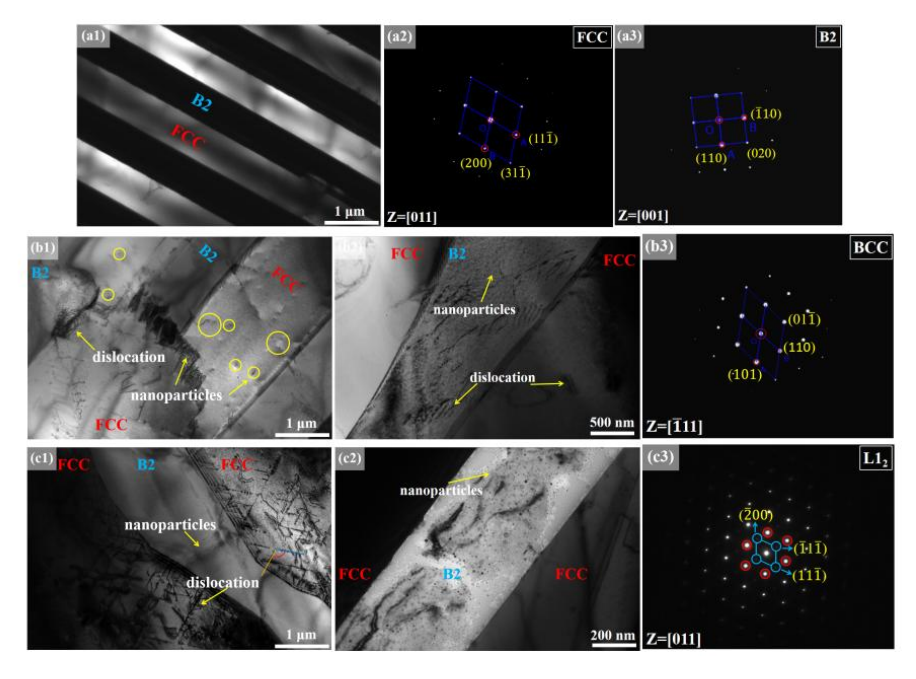


Fig. 5:.TEM images of EHEA samples: (a1) as-cast; (a2-a3) diffraction spot image; (e-f) after DCT-12

In order to further reveal the microstructural evolution caused by CDCT treatment, this study utilized TEM to observe the morphology of both the original samples and those after CDCT. Figure 5(a1) displays the transmission electron microscopy image of the original AlCoCrFeNi_{2.1} EHEAs. A small number of dislocations can be observed, which is due to the rapid solidification occurring under the influence of vacuum arc melting on the copper plate and water cooling, resulting in a limited number of dislocations. The selected area electron diffraction (SAED) evidence in Figures 5(a2-a3) confirms that the matrix of the AlCoCrFeNi_{2.1} EHEAs consists of a dual-phase lamellar structure. The lamellar structure labeled 'FCC' exhibits a face-centered cubic structure (along the [011] direction), while the structure labeled 'B2' has a body-centered cubic structure (along the [001] direction). In the CDCT-1 sample (Figures 5b1-b2), an increase in the number of dislocations is observed, though the dislocation density remains low. Initial low-density precipitation phases begin to appear, concentrated within the B2 phase; the SAED in Figure 5(b3) confirms that the precipitate phase is a BCC coherent precipitate, characterized by small sizes with a diameter range of 10-20 nm. In the CDCT-2 sample (Figures 5c1-c2), there is a further increase in the number of dislocations, with a higher dislocation density found in the FCC phase, gradually entangling to form a dislocation network and dislocation wall structures. Concurrently with the presence of precipitate phases in the B2 phase, larger precipitates also emerge in the FCC phase, with SAED results in Figure 5(c3) confirming that this precipitate is of the L1₂ type, having a statistical diameter range between 30-45 nm. Notably, superlattice diffraction spots (marked with circles) appeared in the diffraction patterns of both phases, indicating the formation of ordered L12 and disordered BCC phases within the face-centered cubic and body-centered cubic matrices. This phenomenon has also been reported previously. However, after the samples undergo CDCT, the superlattice diffraction spots in the body-centered cubic (B2) phase become more pronounced, indicating enhancement in the precipitation of the body-centered cubic (BCC) phase.

3.2 Mechanical properties

Table 2 compares the engineering tensile stress-strain curves of the cast state and AlCoCrFeNi_{2.1} EHEAs subjected to different cyclic deformation counts (CDCT) at room temperature. The yield

strength (YTS) of the cast AlCoCrFeNi_{2.1} EHEAs was measured at 400.07 ± 5.52 MPa, with a ultimate tensile strength (UTS) of 974.25 ± 5.15 MPa and a total elongation (TE) of $19.63\% \pm 1.74\%$. Table 2 summarizes the unexpected improvements in strength and ductility of the AlCoCrFeNi_{2.1} EHEAs processed under CDCT-1, CDCT-2, CDCT-3, and CDCT-4, demonstrating an excellent combination of strength and ductility at room temperature. Notably, increasing the number of CDCT cycles facilitated improvements in the combination of strength and ductility.

Tab.2 Nominal composition of the as-cast AlCoCrFeNi2.1 high entropy alloy

Sample	YS (MPa)	UTS (MPa)	UE (%)
AC	400.07±5.52	974.25±5.15	19.63 ± 1.74
CDCT-1	426.24±5.84	1022.61 ± 6.54	21.54±1.65
CDCT-2	449.96 ± 6.20	1062.78 ± 7.32	22.84 ± 2.72
CDCT-3	474.65±5.26	1089.65 ± 6.11	24.57±1.78
CDCT-4	480.97 ± 5.22	1107.18 ± 5.90	24.21 ± 2.23

In the CDCT reinforced AlCoCrFeNi_{2.1} EHEAs, there exists a significant mechanical incompatibility between the FCC phase and the B2 phase. The strength difference between the soft and hard regions leads to heterogeneous deformation, which causes the HDI reinforcement effect. In this study, the BCC precipitate phase and the L12 precipitate phase are unevenly distributed between the FCC phase and the B2 phase. further modulating the overall heterogeneous deformation behavior. Compared to the cast state samples, the CDCT samples exhibit a higher yield strength, despite a lower content of the BCC precipitate phase. This improvement in performance is primarily attributed to the larger hardness difference between the soft and hard regions, thus triggering a significant HDI strengthening effect^[11].

4 Conclusion

In this study, the microstructure and mechanical properties of AlCoCrFeNi_{2.1} EHEA were extensively investigated with varying duration of CDCT. The CDCT process produces high-density dislocations and uniformly distributed precipitates in EHEAs. This method provides a promising design strategy for optimizing the comprehensive mechanical properties of EHEAs. The conclusions are summarized as follows:

(1) CDCT causes dislocations in AlCoCrFeNi_{2.1} EHEAs, and the dislocation density increases with the extension of DCT time. The dislocation density of CDCT-4 increases to a maximum of 8.23×10^{14} m⁻².

- After CDCT-4, The dislocation morphology also changed significantly, and the low-density dislocation lines were entangled together to become dislocation nets networks or dislocation walls.
- (2) CDCT produces precipitates in AlCoCrFeNi_{2.1} EHEAs. The BCC coherent precipitates are formed in the B2 matrix. With the extension of CDCT time, the volume fraction of precipitates increases, and the size of newly formed precipitates decreases significantly.
- (3) AlCoCrFeNi_{2.1} EHEAs achieve the best comprehensive mechanical properties after CDCT-4. The tensile strength is 1107.18 MPa. The plasticity reaches 24.21%, which is 23.33% higher than that of the as-cast state. AlCoCrFeNi_{2.1} EHEAs are more suitable for engineering applications after being strengthened by CDCT process.

References:

- [1] Yeh J W, Chen S K, Lin S J, et al. Nanostructured high-entropy alloys with multiple principal elements: novel alloy design concepts and outcomes[J]. Advanced engineering materials, 2004, 6(5): 299-303.
- [2] Cantor B, Chang I T H, Knight P, et al. Microstructural development in equiatomic multicomponent alloys[J]. Materials Science and Engineering: A, 2004, 375: 213-218.
- [3] Lu Y, Dong Y, Guo S, et al. A promising new class of high-temperature alloys: eutectic high-entropy alloys[J]. Scientific reports, 2014, 4(1): 6200.

- [4] Shi P, Ren W, Zheng T, et al. Enhanced strength-ductility synergy in ultrafine-grained eutectic high-entropy alloys by inheriting microstructural lamellae[J]. Nature communications, 2019, 10(1): 489.
- [5] He J Y, Wang H, Huang H L, et al. A precipitation-hardened high entropy alloy with outstanding tensile properties[J]. Acta Materialia, 2016, 102: 187-196.
- [6] Qi H, Li G L, Zhang W, et al. Effect of TiO2 nano-ceramic particles on microstructure and mechanical properties of Al0.4CoCrFe2Ni2 high entropy alloy[J]. China Foundry, 2022, 19(6): 528-534.
- [7] Qi H, Lv Q, Li G, et al. Effect of cryogenic treatment on B2 nanophase, dislocation and mechanical properties of Al1.4CrFe2Ni2 (BCC) high entropy alloy[J]. Materials Science and Engineering: A, 2023, 878: 145183.
- [8] Xie S C, Lv Q Y, Zhang W, et al. Effect of cryogenic treatment on microstructure and mechanical properties of Al0.6CrFe2Ni2 dual-phase high-entropy alloy[J]. Metals, 2023, 13(2): 195.
- [9] Liu B, Han D, Li T, et al. Achieving dislocation-precipitation strengthening synergy in additively manufactured medium-entropy alloy via cyclic deep cryogenic strategy[J]. Scripta Materialia, 2025, 256: 116441.
- [10] Taylor G I. Plastic strain in metals[J]. Journal of the Institute of Metals, 1938, 62: 307-324.
- [11] Zou S, Dong C, Tan X, et al. Mitigating embrittlement of sigma phase in dual-phase high-entropy alloys through heterostructure design[J]. International Journal of Plasticity, 2025: 104272.